Dunn, T. M., Hahn, S., Ogden, S., & Schleif, R. F. (1984) *Proc. Natl. Acad. Sci. U.S.A. 81*, 5017–5020.

Felsenfeld, G., & Hirschman, S. Z. (1965) *J. Mol. Biol. 13*, 407–427.

Fried, M., & Crothers, D. M. (1981) *Nucleic Acids Res. 9*, 6505–6525.

Garner, M. M., & Revzin, A. (1981) *Nucleic Acids Res. 9*, 3047–3060.

Gilbert, W. (1976) in *RNA Polymerase* (Losick, R., & Chamberlin, M., Eds.) pp 193–205, Cold Spring Harbor Laboratory, Cold Spring Harbor, NY.

Irani, M. H., Orosz, L., & Adhya, S. (1983) *Cell (Cambridge, Mass.) 32*, 783–788.

Kolb, A., & Buc, H. (1982) *Nucleic Acids Res. 10*, 473–485.

Kolb, A., Spassky, A., Chapon, C., Blazy, B., & Buc, H. (1983a) *Nucleic Acids Res. 11*, 7833–7852.

Kolb, A., Busby, S., Herbert, M., Kotlarz, D., & Buc, H. (1983b) *EMBO J. 2*, 217–222.

Lowe, P. A., Hager, D. A., & Burgess, R. R. (1979) *Biochemistry 18*, 1344–1352.

Majumdar, A., & Adhya, S. (1984) *Proc. Natl. Acad. Sci. U.S.A. 81*, 6100–6104.

Malan, T. P., & McClure, W. R. (1984) *Cell (Cambridge, Mass.) 39*, 173–180.

Malan, T. P., Kolb, A., Buc, H., & McClure, W. R. (1984) *J. Mol. Biol. 180*, 881–909.

Maniatis, T., Fritsch, E. F., & Sambrook, J. (1982) *Molecular Cloning—A Laboratory Manual*, Cold Spring Harbor Laboratory, Cold Spring Harbor, NY.

Maxam, A. M., & Gilbert, W. (1980) *Methods Enzymol. 65*, 499–560.

McClure, W. R. (1980) *Proc. Natl. Acad. Sci. U.S.A. 77*, 5634–5638.

Musso, R. E., DiLauro, R., Adhya, S., & deCrombrugghe, B. (1977) *Cell (Cambridge, Mass.) 12*, 847–854.

Peterson, M. L., & Reznikoff, W. S. (1985) *J. Mol. Biol. 185*, 535–543.

Roe, J.-H., & Record, M. T., Jr. (1985) *Biochemistry 24*, 4721–4726.

Shanblatt, S. H., & Revzin, A. (1983) *Proc. Natl. Acad. Sci. U.S.A. 80*, 1594–1598.

Sklar, J., Weissman, S., Musso, R. E., DiLauro, R., & deCrombrugghe, B. (1977) *J. Biol. Chem. 252*, 3538–3547.

Spassky, A., Busby, S., & Buc, H. (1984) *EMBO J. 3*, 43–50.

Taniguchi, T., & deCrombrugghe, B. (1983) *Nucleic Acids Res. 11*, 5165–5180.

Taniguchi, T., O'Neill, M., & deCrombrugghe, B. (1979) *Proc. Natl. Acad. Sci. U.S.A. 76*, 5090–5094.

Structural Aspects of the Copper Sites in Cytochrome c Oxidase. An X-ray Absorption Spectroscopic Investigation of the Resting-State Enzyme[†]

Robert A. Scott* and James R. Schwartz

School of Chemical Sciences, University of Illinois, Urbana, Illinois 61801

Stephen P. Cramer

Exxon Research and Engineering, Annandale, New Jersey 08801

Received February 5, 1986; Revised Manuscript Received May 16, 1986

ABSTRACT: Copper K-edge X-ray absorption spectroscopy (XAS) has been used to investigate the structural details of the coordination environment of the copper sites in eight resting-state samples of beef heart cytochrome c oxidase prepared by different methods. The unusual position and structure of the resting-state copper edge spectrum can be adequately explained by the presence of sulfur-containing ligands, with a significant amount of S → Cu(II) charge transfer (i.e., a covalent site). Quantitative curve-fitting analysis of the copper extended X-ray absorption fine structure (EXAFS) data indicates similar average first coordination spheres for all resting-state samples, regardless of preparation method. The average coordination sphere (per 2 coppers) mainly consists of 6 ± 1 nitrogens or oxygens at an average Cu–(N,O) distance of 1.99 ± 0.03 Å and 2 ∓ 1 sulfurs at an average Cu–S distance of 2.28 ± 0.02 Å. Quantitative curve-fitting analysis of the outer shell of the copper EXAFS indicates the presence of a Cu⋯Fe interaction at a distance of 3.00 ± 0.03 Å. Proposed structures of the two copper sites based on these and other spectroscopic results are presented, and differences between our results and those of other published copper XAS studies [Powers, L., Chance, B., Ching, Y., & Angiolillo, P. (1981) *Biophys. J. 34*, 465–498] are discussed.

Cytochrome c oxidase (ferrocytochrome c/O_2 oxidoreductase, EC 1.9.3.1) catalyzes the final step of mitochondrial respiration, the four-electron reduction of O_2 using reducing equivalents from the electron transport chain.[1] The enzyme utilizes four spectroscopically distinct redox-active metal sites to accomplish this task. Two iron atoms are present in the form of a heme a prosthetic group and are labeled heme a and heme a_3, forming the basis for the alternative name of this enzyme, cytochrome aa_3. Two copper atoms are also asso-

[1] For an excellent review of cytochrome c oxidase, see Wikström et al. (1981).

ciated with the enzyme and will be labeled Cu_A and Cu_B^2 from here on. The iron of heme a_3 (Fe_{a3}) and Cu_B are present as a magnetically interacting binuclear site at which O_2 binding and reduction occurs. Heme a and Cu_A are magnetically (and probably physically) isolated and are thought to act as "electron reservoirs" to feed reducing equivalents to the O_2-interaction site.

Bovine heart cytochrome c oxidase is aerobically isolated in the fully oxidized state (referred to herein as the "resting state"), which is then capable of accepting four electrons (one per metal site) to generate the fully reduced enzyme. Reoxidation of the fully reduced enzyme by O_2 generates a form of the fully oxidized enzyme which is spectroscopically distinct from the resting state. Immediately following reoxidation, the enzyme is found to exist in an activated state exhibiting enhanced turnover rates, a state that is referred to as the "pulsed" enzyme form (Colosimo et al., 1981). Previous studies had identified an "oxygenated" enzyme form which persists at longer time following O_2 reoxidation of the reduced enzyme (Oril & Okunuki, 1963). Although the majority of spectroscopic investigations of cytochrome c oxidase (including the present one) have been performed on the resting-state form, it is now clear that this is a relatively inactive enzyme form, requiring reduction before becoming catalytically competent (Brunori et al., 1979). The elucidation of the structural basis for this required activation is the goal of current spectroscopic studies on the resting-state enzyme, which must then be accompanied by parallel studies on the activated enzyme forms. We report here a summary of recent results in our study of resting-state cytochrome c oxidase using the technique of X-ray absorption spectroscopy (XAS) to study the structures of the copper sites. We are also currently involved in similar studies on the oxygenated enzyme form.

Investigations of resting state cytochrome c oxidase have been hampered in the past by irreproducibility, especially among enzyme samples prepared by different methods. This irreproducibility is partly due to enzyme heterogeneity in the resting state. At least three separate enzyme forms are present in resting-state samples, with different preparations exhibiting different proportions of the various forms (Brudvig et al., 1981). The extent to which this heterogeneity is reflected in the structures of the metal sites of cytochrome c oxidase is investigated herein by comparison of copper XAS data of resting-state derivatives prepared by various methods.

Previous work has established some details concerning the structural environments of the copper sites in cytochrome c oxidase. Cu_A exhibits the unique $g = 2$ signal in the EPR spectrum of the resting-state enzyme. The small copper hyperfine splitting observed by low-frequency EPR (Froncisz et al., 1979) and by ENDOR (Hoffman et al., 1980) has been ascribed to a significant delocalization of unpaired spin onto sulfur-containing ligands, suggesting the existence of considerable S → Cu charge transfer. The existence of sulfur-containing ligands in the copper-coordination sphere was first directly demonstrated by EXAFS (Scott et al., 1981). Labeling studies on yeast cytochrome c oxidase have provided evidence for the coordination of at least one histidine and one cysteine at the Cu_A site (Blair et al., 1983). Much less is known about the coordination environment of Cu_B, since its magnetic coupling to Fe_{a3} results in an EPR-silent state. Other

XAS studies have suggested that Cu_B may be a blue copper and may be bridged to Fe_{a3} through a sulfur-containing ligand (Chance & Powers, 1985; Powers et al., 1981). These assignments are reexamined in light of the Cu XAS data presented here.

MATERIALS AND METHODS

Enzyme Sample Preparation. Copper XAS data were collected on eight separate samples of resting-state cytochrome c oxidase prepared by four methods in six different laboratories. Four of the samples were prepared by the Hartzell/Beinert method [Procedure I of Hartzell et al. (1978)]: Samples HB/Ua and HB/Ub were prepared in our laboratory in Urbana, sample HB/M was prepared in the laboratory of H. Beinert in Madison, and sample HB/P was prepared in the laboratory of S. I. Chan in Pasadena. Samples K/Bm and K/Bd were prepared by the King method [Procedure II of Hartzell et al. (1978)] in the laboratory of A. Azzi in Bern. Sample K/Bm was prepared by methods that yield the "monomer" form, and sample K/Bd was prepared by methods that yield the "dimer" form of the enzyme (Nalecz et al., 1983). Sample vB/A was prepared by the van Buuren method [Procedure III of Hartzell et al. (1978)] in the laboratory of B. F. van Gelder in Amsterdam and was obtained through H. Beinert. Sample Y/E was prepared by the Yonetani method (Yonetani, 1961) in the laboratory of M. T. Wilson in Essex.

X-ray Absorption Data Collection. All XAS data were collected at the Stanford Synchrotron Radiation Laboratory (SSRL) on wiggler beam-line side station VII-3 under dedicated operating conditions (3.0 GeV, 60–70 mA) using Si[220] monochromator crystals. For high-resolution edge scans, the premonochromator vertical-beam aperture was set to 1 mm, whereas a 2-mm aperture was used for all EXAFS scans. The data were collected over an energy range of 8700–9700 eV, with the upper limit being dictated by the presence of zinc (with a K absorption edge at 9661 eV) in every sample. Each scan lasted 25–30 min, with 7–15 scans being averaged for each sample. The data were collected as fluorescence excitation spectra using an array of 17 NaI(Tl) scintillation detectors and Ni filters similar to the setup previously described (Cramer & Scott, 1981). The data from each detector were collected separately and then averaged together by using a weighting scheme that accounts for the differences in signal-to-noise ratio for different detectors at different positions (Scott, 1985).

The concentrated (ca. 2 mM in Cu) samples were contained in rectangular lucite cells 2.5 cm long with a 0.2 × 0.4 cm cross section. The cells were positioned with one of the 2.5 × 0.4 cm sides facing the beam. This side was made up of a single thickness of 0.001-in. Mylar tape as an X-ray transparent window. The long axis of the cell was horizontal and at 45° to the beam propagation direction so that the scintillation detectors also "viewed" the Mylar face. The Lucite/Mylar cells were designed with an outside dimension compatible with a standard X-band EPR cavity dewar. Once filled with sample and capped, the cell was quickly frozen in liquid nitrogen, and a Nylon extension was attached to the cell by means of a small threaded hole in the cap. This assembly mimicked a standard EPR tube and was used to examine the EPR of the sample both before and after XAS data collection. Typically, samples in cells were stored in liquid nitrogen (77 K), examined by EPR at 10 K, shipped to SSRL at 77 K, examined by XAS at either 4 K (samples HB/Ub, K/Bm, K/Bd, Y/E) or 190 K (samples HB/Ua, HB/M, HB/P, vB/A), shipped back to Urbana at 77 K, and reexamined by EPR at 10 K. As previously reported, although EPR spectra indicated the pro-

---

[2] Abbreviations: EPR, electron paramagnetic resonance; ENDOR, electron–nuclear double resonance; EXAFS, extended X-ray absorption fine structure; XAS, X-ray absorption spectroscopy; Cu_A, EPR-detectable copper site; Cu_B, EPR-undetectable copper site; Fe_{a3}, iron associated with the heme of cytochrome a_3.

duction of radicals during X irradiation, no redox changes in the cytochrome c oxidase metal sites were observed as long as XAS data collection was performed below ca. 200 K (Scott et al., 1984). The temperature of the samples during XAS data collection was maintained by the use of a liquid helium cryostat (Oxford Instruments, Model CF1208) that was custom-designed for fluorescence excitation XAS measurements. This is a continuous-flow cryostat with X-ray transparent, vacuum-tight aluminized Mylar windows and the sample situated in atmospheric pressure cold helium gas (for quick sample change).

Data Reduction and Analysis. Data reduction (i.e., extraction of the EXAFS data from the raw XAS data) was accomplished by our standard techniques (Scott, 1985). After energy calibration of individual scans using the internal calibration method (Scott, 1982) with a copper foil reference (first inflection point at 8980.3 eV) and the averaging of scans as described above, the background was removed by fitting a second-order polynomial to the data between 9050 and 9650 eV and subtracting a constant from it selected so that the polynomial passed through the data just before the Cu K absorption edge. After subtraction of the resulting polynomial, a third-order spline was fit to the data between 9035 and 9650 eV with spline nodes at 9180 and 9400 eV. This spline was subtracted from the data, and the resultant was normalized by dividing by the Cu atomic falloff as modeled by the Victoreen equation (MacGillavry & Rieck, 1968), multiplied by a factor that forced the falloff curve to match the spline polynomial at 9000 eV (defined as $k = 0$). This factor corrects for any differences in edge height (i.e., concentration) from one sample to another. The resultant data are the EXAFS (χ), which are usually treated as a function of the photoelectron wave vector (k, units of Å^{-1}) rather than energy.

For the curve-fitting analyses, the following theoretical expression for the EXAFS was used:

$$\chi(k) = \sum_s \frac{B_s N_s |f_s(\pi,k)|}{k R_{as}^2} \exp(-2\sigma_{as}^2 k^2) \sin [2k R_{as} + \alpha_{as}(k)]$$

(1)

In this expression, subscript a stands for absorber and s for scatterer. The summation is over all shells of scatterers. For each shell of scatterers, s, N_s is the number of scatterers at an average distance R_{as} from the absorbing Cu atom. σ_{as} is the root mean square deviation in R_{as}, which includes both static (from small differences in R_{as} among the scatterers within the shell) and dynamic (from vibrational motion) contributions (Scott, 1985). Curve-fitting is performed by the use of a Cu coordination environment hypothesis in terms of a number of shells of atoms, followed by use of eq 1 to simulate the expected EXAFS. The fit of this simulated EXAFS to the observed EXAFS is then adjusted by allowing some of the N_s, R_{as}, and σ_{as} values for each shell to vary in a nonlinear least-squares optimization. In the fits reported herein, N_s for each shell is chosen as some integer (per two copper atoms), and R_{as} and σ_{as} are varied in each shell. In each shell, the type of scattering atom (e.g., C, N, O, S) is chosen by selection of the appropriate backscattering function, which appears in eq 1 as amplitude $[B_s |f_s(\pi,k)|]$ and phase $[\alpha_{as}(k)]$ components. (B_s is a scale factor that is used to correct theoretical amplitude functions. Our use of empirical functions as described below allows us to fix B_s at unity.) In general, for each absorber–scatterer (a–s) pair of interest, the backscattering function must be known. Although methods are available for calculating this function ab initio (Teo & Lee, 1979), we chose to empirically measure this function by examining the Cu EX-

AFS of structurally characterized compounds containing a shell of the appropriate scatterer. Extraction of the amplitude and phase components of the backscattering function is accomplished by complex Fourier back-transformation, described in detail elsewhere (Scott, 1985).

Individual shells of EXAFS (i.e., single terms of the sum of eq 1) can sometimes be isolated from other shells by the Fourier transform (FT) technique. Fourier transformation of $\chi(k)$ data yields a set of peaks in the inverse (R', units of Å) space, each peak falling at an R' value related to the frequency term ($2k R_{as}$) of eq 1. Due to the phase shift $\alpha_{as}(k)$, the R' of a FT peak is related to R_{as} for that shell by $R_{as} \cong R' + \Delta$, where $\Delta \cong 0.2$–0.5 Å. If an FT peak is separated well from other peaks, it may be filtered out and back-transformed to k-space, yielding $\chi'(k)$ data, referred to as Fourier-filtered EXAFS data. Fourier filtering is the basis of the complex back-transform technique for generating empirical backscattering functions (Lee et al., 1981), and it is also useful for separating out shells of scatterers for detailed curve-fitting. In the fits performed on the cytochrome c oxidase Cu EXAFS, the first two major shells of scattering (forming the average first coordination sphere) were Fourier-filtered together. The "third shell" (i.e., the third peak in the Fourier transform) was Fourier-filtered by itself and curve-fit separately.

A number of structurally characterized "model" compounds were examined by Cu EXAFS for extraction of empirical backscattering functions for curve-fitting the cytochrome c oxidase data. For Cu–N scattering, EXAFS data collected by fluorescence excitation on a solution sample of [Cu(imidazole)$_4$]$^{2+}$, prepared by literature methods (McFadden et al., 1976), were used along with transmission data on a powder sample of Cu([14]aneN$_4$)(SC$_6$F$_5$)$_2$ ([14]aneN$_4$ = 1,4,8,11-tetraazacyclotetradecane) (Addison & Sinn, 1983), which was kindly donated by A. W. Addison. The single first-shell Cu–N FT peak from each of these data sets was filtered out and back-transformed to yield amplitude and phase components of the backscattering functions, which were then averaged and used for the cytochrome c oxidase curve-fitting. Similarly isolated first-shell Cu–S interactions were used from EXAFS data on solid samples of [(n-C$_4$H$_9$)$_4$N]$_2$[Cu(mnt)$_2$] (mnt = maleonitriledithiolate) prepared by the published procedure (Davison & Holm, 1967) and [Cu([14]aneS$_4$)](ClO$_4$)$_2$ ([14]aneS$_4$ = 1,4,8,11-tetrathiacyclotetradecane) (Glick et al., 1976), a gift from D. B. Rorabacher, to derive averaged backscattering functions for Cu–S curve-fitting. Since one aspect of this study involved looking for the presence of Fe$_{a_3}$ in the Cu$_B$ outer coordination sphere, a model for Cu···Fe scattering was needed. For this we used the Fe$_2$Cu trinuclear compound [Fe(TPP)]$_2$[Cu(mnt)$_2$] (TPP = *meso*-tetraphenylporphyrin) (Elliott & Akabori, 1982), a gift from C. M. Elliott. The structure of this compound was assumed to be analogous to the closely related Fe$_2$Cu$_2$ compound (Schauer et al., 1984) with an average Cu···Fe distance of 3.89 Å. The Cu EXAFS of the Fe$_2$Cu compound (at 4 K) exhibits an FT peak at $R' = 3.51$ Å which is not present in the FT of [Cu(mnt)$_2$]$^{2-}$ and which is thus assignable to the Cu···Fe interactions. This FT peak was Fourier-filtered and a Cu···Fe backscattering function extracted for use in curve-fitting of the cytochrome c oxidase data. An empirical backscattering function for Cu···C (outer shell) interactions was derived by Fourier filtering the FT peak corresponding to the Cu···C shell of [Cu(mnt)$_2$]$^{2-}$. The Cu···C distance in this compound is 3.12 Å (Plumlee et al., 1975), giving rise to an FT peak at $R' = 2.94$ Å.
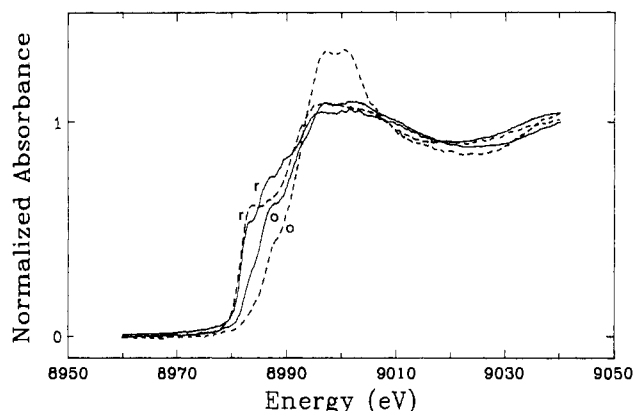
FIGURE 1: Comparison of copper K absorption edge spectra for cytochrome c oxidase (—) and bovine plasma amine oxidase (- - -). In each case, o is the spectrum for the oxidized enzyme, r is the spectrum for reduced. The resting state (o) spectrum for cytochrome c oxidase is from sample K/Bm, while the reduced (r) spectrum is from sample HB/M. The energy difference between the oxidized amine oxidase and resting-state cytochrome c oxidase edges is indicative of the more covalent nature of the Cu(II) sites in cytochrome c oxidase.

Estimation of the error associated with each variable parameter in the curve-fitting procedure was accomplished as follows. First, a modified goodness-of-fit statistic (defined as f) was used:

$$f \equiv \frac{\{\sum_i [k^3(\chi_{obsd}{}^{(i)} - \chi_{calcd}{}^{(i)})]^2/N\}^{1/2}}{(k^3\chi)_{max} - (k^3\chi)_{min}}$$

This statistic differs from the usual one in that it is normalized for differences in the magnitude of the $k^3\chi$ data from one spectrum to another. For a particular data set, each parameter was varied in turn, keeping all other parameters fixed at their best-fit values, and f was calculated to yield a unidimensional projection of the error hypersurface. The error in the parameter was estimated to be the change necessary to increase the value of f by an amount Δf from its minimum value. The value of Δf was 0.02, empirically chosen to give reasonable errors in a wide variety of systems.

For comparison with resting-state cytochrome c oxidase, the copper K absorption edge spectra of a few model compounds were recorded. Na[Cu(MPG)(H$_2$O)] [MPG = (mercaptopropionyl)glycine] was prepared by the published method (Sugiura et al., 1975). Although the crystal structure of this compound is not available, our Cu EXAFS analysis supports the proposed CuNSO$_2$ coordination [3 (N, O) at 1.98 Å, 1 S at 2.30 Å]. {Cu[(prp)$_2$en]Fe(hfa)$_2$} [(prp)$_2$en is the Schiff base made from 2 mol of 2-hydroxypropiophenone and 1 mol of ethylenediamine; hfa = hexafluoroacetylacetonate] was a gift from E. Sinn. [Cu(pmaS)](BPh$_4$) [pmaS = (2-pyridylmethyl)bis[2-(ethylthio)ethyl]amine] (Karlin et al., 1980) was a gift from K. D. Karlin.

RESULTS AND DISCUSSION

Copper X-ray Absorption Edges. Ever since the first copper XAS work on cytochrome c oxidase (Hu et al., 1977a,b), the position and shape of the Cu K edge of resting-state cytochrome c oxidase have been the subject of controversy. The main reason for this controversy is that the position of the edge falls at a significantly lower energy than the Cu K edges of "normal" Cu(II) compounds. An example of this difference is illustrated in Figure 1, where the edges of resting-state and dithionite-reduced cytochrome c oxidase are compared with the edges of oxidized and dithionite-reduced bovine plasma
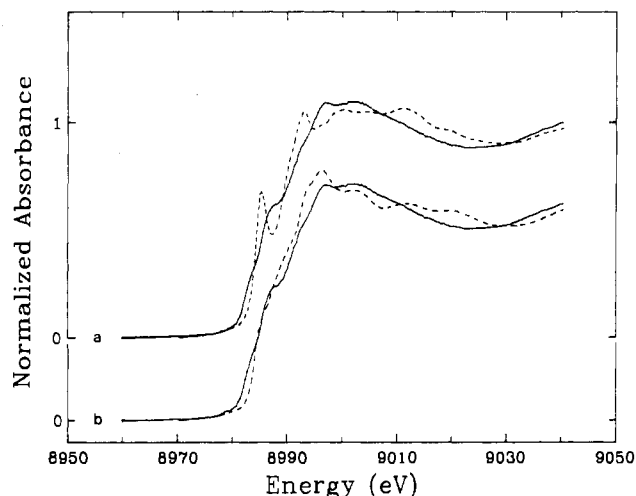

FIGURE 2: Comparison of the copper K absorption edge spectrum for resting-state cytochrome c oxidase with edge spectra for two Cu(II) complexes with sulfur ligation. (a) Resting state cytochrome c oxidase (—) and [(n-C$_4$H$_9$)$_4$N]$_2$[Cu(mnt)$_2$] (mnt = maleonitriledithiolate) (- - -). (b) Resting-state cytochrome c oxidase (—) and [Cu([14]-aneS$_4$)](ClO$_4$)$_2$ ([14]aneS$_4$ = 1,4,8,11-tetrathiacyclotetradecane) (- - -). The unusually low-energy position of the resting-state edge can be explained by the presence of Cu^{II}–S ligation.

amine oxidase. The position of the resting state edge led Hu et al. (1977a) to conclude that one of the copper sites in the resting-state enzyme was in the Cu(I) state. [The sample used in that study was later suggested to be partially reduced by X irradiation (Powers et al., 1979), but their resting-state edge looks very similar to several that have been reported since (Powers & Chance, 1984; Scott, 1982), including that illustrated in Figure 1.] The Cu(II) coordination environment in oxidized amine oxidase is known to consist solely of "hard" ligands (e.g., N, O) (Scott & Dooley, 1985). For "soft" ligands (e.g., S), the Cu(II) edge position would be expected to fall at lower energy since the edge position is a measure of effective charge density at the copper and some amount of S → Cu charge transfer is expected. The comparison in Figure 2 indicates that this explanation is essentially correct. The edges of [Cu([14]aneS$_4$)]$^{2+}$ and [Cu(mnt)$_2$]$^{2-}$ occur at significantly lower energy than the edge of oxidized amine oxidase. Thus, one does not have to propose a Cu(I) oxidation state for either copper site in order to explain the resting-state edge position; the presence of sulfur ligation to copper(II) is sufficient.

To further illustrate this point, we have measured Cu K edge spectra for a series of Cu(II) and Cu(I) model compounds and attempted to simulate the essential features for the resting state edge by averaging the edges of two model compounds. Figure 3 shows two such simulations. In Figure 3b, the edge of resting-state cytochrome c oxidase is compared with a simulated edge consisting of a 50:50 combination of the edges of [Cu([14]aneN$_4$)](SC$_6$F$_5$)$_2$ [a Cu(II) complex with a square planar array of N ligands and two axial thiolates with long Cu–S distances (Addison & Sinn, 1983)] and Na[Cu(MPG)(H$_2$O)] [a Cu(II) complex with NSO$_2$ coordination (Sugiura et al., 1975)]. Figure 3d compares the resting-state edge with a simulated edge consisting of a 50:50 combination of [Cu(pmaS)](BPh$_4$) [a Cu(I) complex with N$_2$S$_2$ coordination (Karlin et al., 1980)] and {Cu[(prp)$_2$en]Fe(hfa)$_2$} [a Cu(II)/Fe(III) binuclear complex with CuN$_2$O$_2$ coordination]. In each case, the position and other features of the resting-state cytochrome c oxidase edge are adequately simulated, assuming either a Cu(I) assignment for one site or Cu(II)–S ligation.

This approach to simulating the resting-state edge is identical with the "site modeling" approach used by Powers et al.
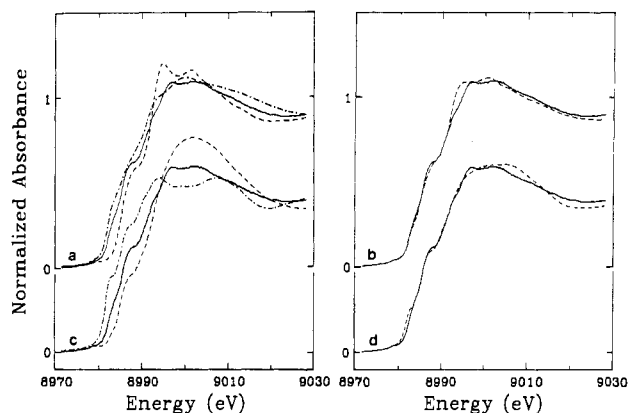
FIGURE 3: Simulation of the resting-state cytochrome c oxidase copper K edge spectrum using combinations of edge spectra from "model" compounds. In each case, the solid line is the resting-state edge spectrum. (a) Edge spectra for $[Cu^{II}([14]aneN_4)](SC_6F_5)_2$ ([14]-aneN$_4$ = 1,4,8,11-tetraazacyclotetradecane)(---) and Na[Cu^{II}-(MPG)(H$_2$O)] (MPG = (mercaptopropionyl)glycine) (─·─). (b) Simulated edge for a 50:50 combination of the two edges described in (a) (---). (c) Edge spectra for {Cu^{II}[(prp)$_2$en]Fe^{III}(hfa)$_2$} (prp = 2-hydroxypropiophenone; en = ethylenediamine; hfa = hexafluoro-acetylacetonate) (---) and [Cu^{I}(pmaS)](BPh$_4$) [pmaS = (2-pyridylmethyl)bis[2-(ethylthio)ethyl]amine] (─·─). (d) Simulated edge for a 50:50 combination of the two edges described in (c) (---). The basic position and features of the resting-state cytochrome c oxidase edge can be simulated by using either a Cu(II), Cu(II) or a Cu(I), Cu(II) combination, as long as some sulfur ligation is assumed.

(1979) in their analysis of the copper edges of cytochrome c oxidase. In that study, this approach was used to assign the structural environment of the Cu$_A$ and Cu$_B$ sites by using the copper edge of stellacyanin and other model compounds. The results were used to support the conclusion that Cu$_B$ was a blue copper-like site. The simulations in Figure 3 indicate the

problem with such an approach. An assignment of structures by site modeling can never be unique since another pair of model edges can always be envisioned to add together to give an equally good simulation with a different set of edge features being contributed by each model. Figure 3b,d would result in two completely different structural assignments for the Cu$_A$ and Cu$_B$ sites, with no reason to believe one over the other. The resting-state copper edges thus give no unequivocal evidence for the existence of a blue copper site in cytochrome c oxidase.

Copper EXAFS. A completely analogous argument can be made against the use of a "site modeling" approach in the EXAFS region (Powers et al., 1981). In fact, since the overall EXAFS is simply a sum of terms each resulting from an individual scattering (ligand) atom in *both* copper sites, it is inherently impossible to assign these scatterers to one site rather than the other, based on the EXAFS of a single derivative. Arbitrarily choosing a site model that incorporates a certain subset of these scatterers automatically assigns the rest of the scatterers to the other site. Such a solution cannot be unique since the initial site model could have been chosen to incorporate a different subset of scatterers, resulting in completely different structural assignments for both sites. Our approach involves using curve-fitting to determine the overall average coordination of both copper sites in any particular enzyme derivative (as discussed below for the resting state). Comparison with derivatives in which a single copper site has been chemically perturbed (e.g., by a redox change or ligand binding) should then allow assignment of some of the copper ligands to specific sites.

Figure 4 shows the raw EXAFS data [plotted as $k^3\chi(k)$] for each of the eight resting-state samples examined in this study. Figure 5 shows the Fourier transforms for these eight samples. The signal-to-noise ratio exhibited in these figures
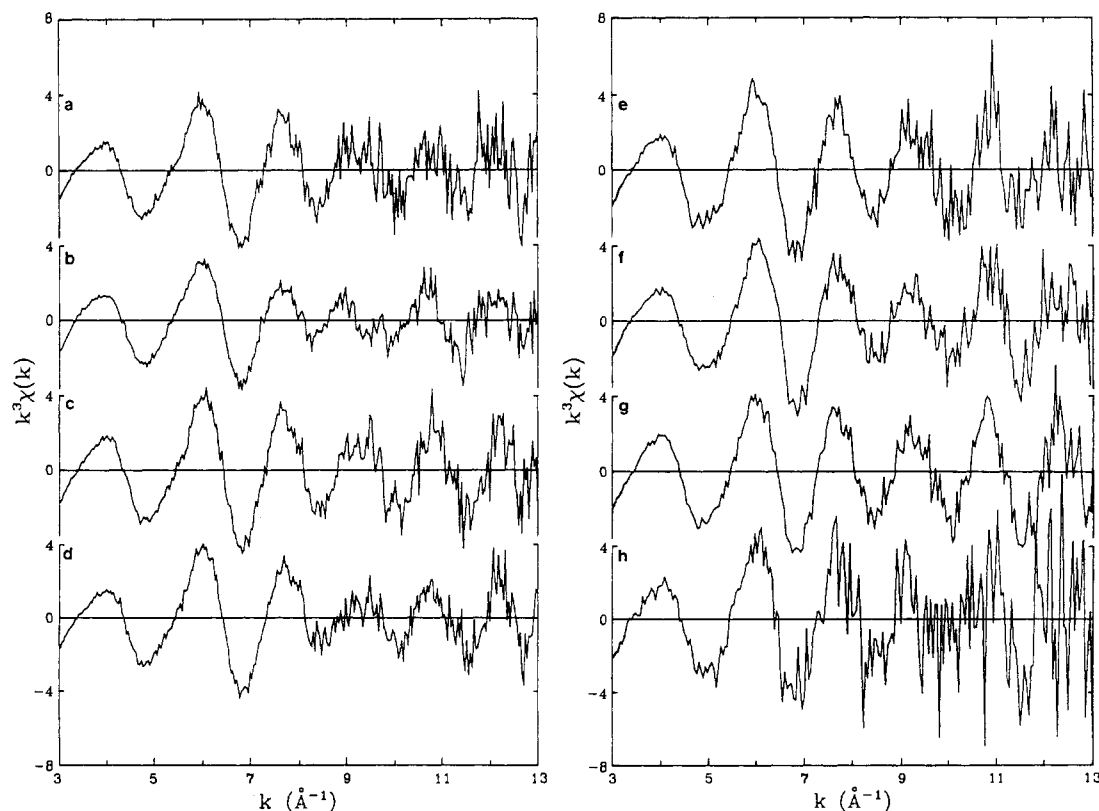

FIGURE 4: Copper EXAFS spectra of the eight resting-state cytochrome c oxidase samples examined. The samples are (a) HB/Ua, (b) HB/M, (c) HB/P, (d) vB/A, (e) HB/Ub, (f) K/Bm, (g) K/Bd, and (h) Y/E. The data in (a)–(d) were recorded at 190 K and the data in (e)–(h) were recorded at 4 K.
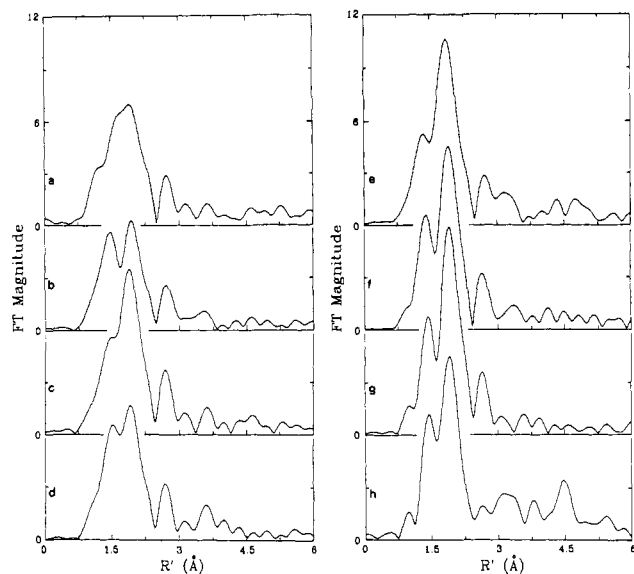
FIGURE 5: Fourier transforms (k = 3.0–13.0 Å^{-1}, k^3 weighted) of copper EXAFS of the eight resting-state samples examined. The samples are the same as listed in the caption of Figure 4.

is typical for fluorescence excitation data on 2 mM Cu samples. In general, the FT consists of two major peaks at $R' \cong 1.5$, 1.9 Å and a smaller peak at $R' \cong 2.7$ Å. Except for a peak sometimes discernible at $R' \cong 3.5$ Å, features beyond this are much less reproducible and are probably assignable to noise. The FT peak at $R' = 3.5$ Å is probably derived from scattering by the outer atoms (N_1, C_5) of imidazoles but has not been analyzed in detail. The resolution of the two main peaks varied considerably from sample to sample, especially for the data at 190 K. One of the main differences between the Cu EX-AFS data published by the two groups working on cytochrome c oxidase is the lack of resolution of these FT peaks in the data published by Powers et al. (1981). The resolution of these FT peaks is simply dependent on the magnitude of the beat pattern in the EXAFS data (Figure 4) and does not necessarily imply a significant structural difference (vide infra). The main difference between the data at 190 K and the data at 4 K is the increase in magnitude of the second major FT peak (at $R' \cong 1.9$ Å) in the 4 K data. This is attributable to a decrease in the vibrational contribution to ρ_{as}^2 for this shell at lower temperature and supports the assignment of this shell to a Cu–S interaction (vide infra).

Curve-fitting was performed in order to determine the metrical details of the average copper coordination sphere in the various preparations of resting-state cytochrome c oxidase. Fourier filtering was used to isolate shells of scattering atoms for these fits. Since the first two FT peaks were sometimes unresolved (see Figure 5), they were filtered out and curve-fit together as exemplified in Figure 6. Figure 6a shows the raw EXAFS data of sample K/Bd (Figure 4g), and Figure 6b is the FT (Figure 5g). The dashed line in Figure 6b represents the window used to select out the two major peaks (representing the average copper first coordination sphere). Back-transformation of these two peaks yield the filtered data [$\chi'(k)$] shown as the solid line in Figure 6c. The filtered data for each sample were then curve-fit by using Cu–N and Cu–S backscattering functions derived as detailed in Materials and Methods. For each fit, a coordination number (per copper) was chosen for each shell to be integer or half-integer (since there are two coppers); then R_{as} and σ_{as}^2 for each shell were optimized in a least-squares fashion. As expected, the best fit always required one shell of Cu–N and one shell of Cu–S
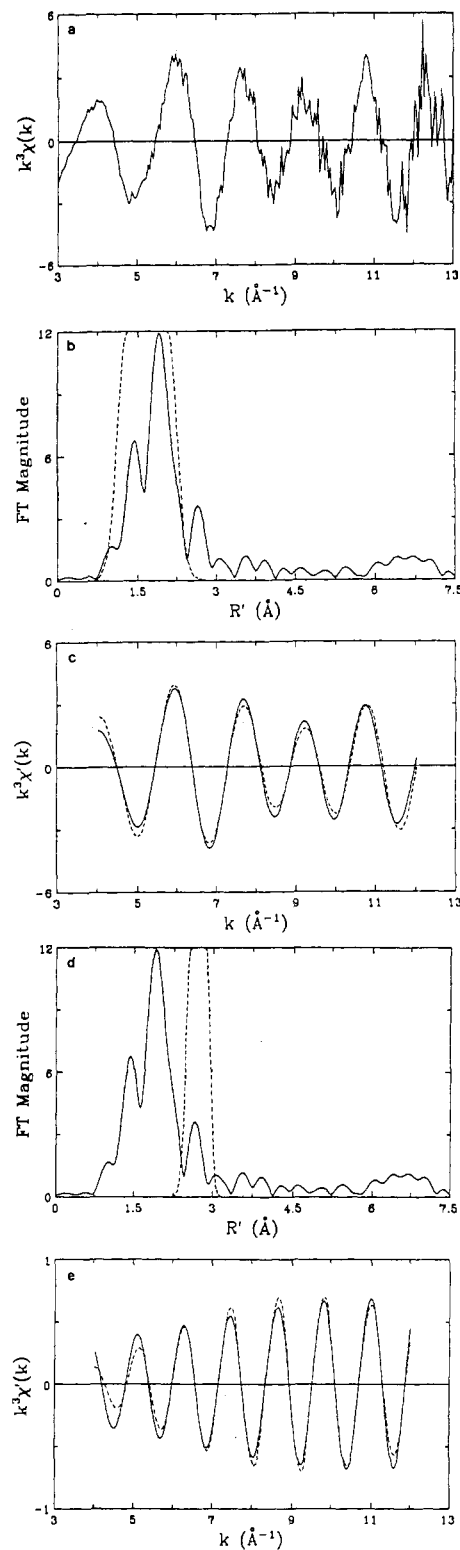

FIGURE 6: Example of Fourier filtering and curve-fitting of the various shells of copper ligands in resting-state cytochrome c oxidase sample K/Bd. (a) Raw copper EXAFS data (same as Figure 4 g). (b) Fourier transform (FT) of (a) (same as Figure 5g) with Fourier filter window (- - -) used to extract the first-shell peaks. Multiplication of the FT by this window followed by back-transformation leads to the filtered [$\chi'(k)$]data shown in (c) (—). The best-fit simulation using Cu–(N,O) and Cu–S shells (see Table I) is also shown in (c) (- - -). (d) The same FT as in (b) with the filter window (- - -) used to extract the third-shell-peak (at $R' \cong 2.7$ Å). Back-transformation yields the filtered data in (e) (—). The best-fit simulation of this shell using Cu···C and Cu···Fe shells (see Table II) is also shown in (e) (- - -). [Note the difference in scales between (c) and (e).]

Table I: Curve-Fitting Results for the First Coordination Sphere of Resting-State Cytochrome c Oxidase Samples[a]

sample	T (K)	Cu-(N,O)			Cu-S			f'
		N_s	R_{as} (Å)	$\Delta\sigma_{as}^2$ (Å²)	N_s	R_{as} (Å)	$\Delta\sigma_{as}^2$ (Å²)	
HB/Ua	190	(3)[b]	2.02 ± 0.03	0.0080 + 0.0059 / − 0.0030	(1)	2.29 ± 0.02	0.0005 + 0.0024 / − 0.0016	0.0505
HB/M	195	(3)	1.98 ± 0.02	0.0070 + 0.0043 / − 0.0023	(1)	2.30 ± 0.02	0.0002 + 0.0021 / − 0.0014	0.0450
HB/P	190	(3)	2.00 ± 0.03	0.0069 + 0.0053 / − 0.0027	(1)	2.28 ± 0.02	−0.0017 + 0.0018 / − 0.0012	0.0458
vB/A	190	(3)	2.00 ± 0.02	0.0055 + 0.0043 / − 0.0022	(1)	2.28 ± 0.02	−0.0007 + 0.0020 / − 0.0014	0.0429
HB/Ub	4	(3)	2.00 ± 0.04	0.0077 + 0.0072 / − 0.0032	(1)	2.27 ± 0.02	−0.0021 + 0.0020 / − 0.0013	0.0566
K/Bm	4	(3)	1.98 ± 0.03	0.0061 + 0.0052 / − 0.0026	(1)	2.27 ± 0.01	−0.0026 + 0.0016 / − 0.0011	0.0416
K/Bd	4	(3)	1.98 ± 0.02	0.0060 + 0.0044 / − 0.0024	(1)	2.28 ± 0.01	−0.0031 + 0.0013 / − 0.0010	0.0383
Y/E	4	(3)	1.99 ± 0.02	0.0045 + 0.0040 / − 0.0022	(1)	2.28 ± 0.02	−0.0024 + 0.0019 / − 0.0011	0.0372

[a] N_s is the coordination number per copper; R_{as} is the copper-scatterer distance; $\Delta\sigma_{as}^2$ is a relative mean square deviation in R_{as}, $\Delta\sigma_{as}^2 = \sigma_{as}^2$ (sample) − σ_{as}^2 (reference), where the reference is $[Cu(imidazole)_4]^{2+}$ at 4 K for Cu-(N,O) and $[Cu(mnt)_2]^{2-}$ at 4 K for Cu-S. [b] Numbers in parentheses were not varied during optimizations.

interactions. (It should be noted that since N backscattering is difficult to distinguish from O or C backscattering, the coordination numbers given for N could represent combinations of N and O or C scatterers, although C is chemically less reasonable.) To reduce the number of variables, it was assumed that the average copper coordination number was 4 [i.e., $N_s(N) + N_s(S) = 4$]. Within this constraint, the combination $N_s(N) = 3$ and $N_s(S) = 1$ gave the best fit for each sample [these numbers probably have an error of ±25% (Scott, 1985)]. The results of the fits for this composition of N and S ligands are summarized in Table I, in which coordination numbers are given on a per copper basis.

The main differences among the curve-fitting results for different samples lie in the $\Delta\sigma_{as}^2$ values. We suggest a visual method for determining whether these differences are significant. Figure 7 shows the EXAFS simulations derived from the fits in Table I plotted on top of one another (for each temperature). Since the differences among the fits for a given temperature are not significantly greater than the noise in the raw data (cf., Figure 4), we conclude that any differences in the copper first coordination spheres for the various resting-state samples examined are within our experimental error. Note that this conclusion was reached despite what *appear* to be significant differences among the Fourier transforms (Figure 5) for these samples. Thus, simple observation of FT differences does not necessarily imply *significant* structural differences.

Within experimental error, regardless of preparation, the major first coordination sphere copper ligands in resting-state cytochrome c oxidase consist of 6 ± 1 N- (or O-)containing ligands (per two coppers) at an average Cu-(N,O) distance of 1.99 ± 0.03 Å and 2 ∓ 1 S-containing ligands at an average Cu-S distance of 2.28 ± 0.02 Å. The σ_{as}^2 value for the Cu-(N,O) shell is significantly larger than that for $[Cu(im-idazole)_4]^{2+}$ and is temperature-independent (see Table I). This indicates that the Cu-(N,O) distances are disordered about the average. A simple calculation assuming two sets of three each Cu-(N,O) interactions at two different distances suggests a static ΔR of ∼0.15 Å. The σ_{as}^2 value for the Cu-S shell is lower at 4 K than at 190 K, indicating a substantial vibrational component. This is usually observed for Cu-S interactions and reflects the lower frequency of a Cu-S stretching vibration compared to that for Cu-N or Cu-O. Our previous work has shown that the Cu-S shell is significantly altered upon reduction of Cu_A (in both mixed valence formate
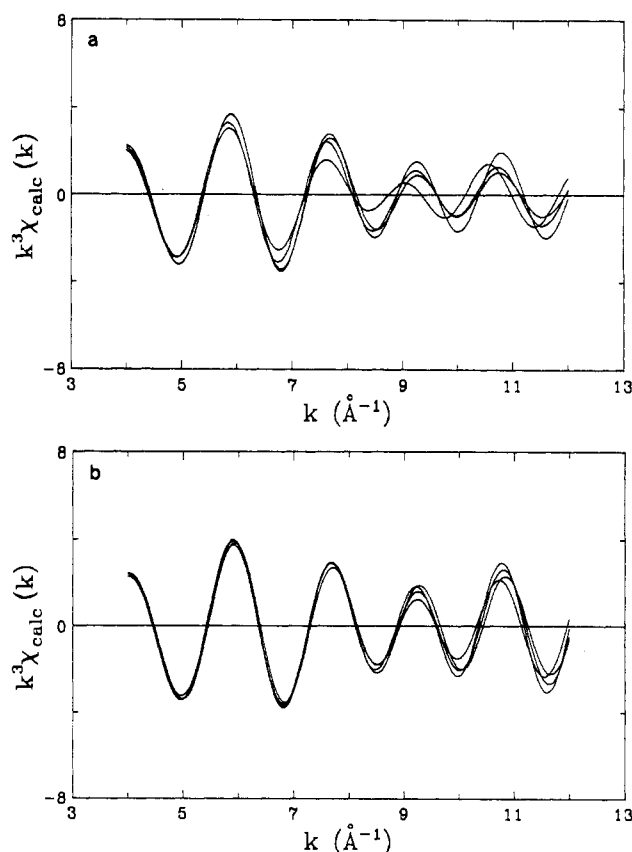

FIGURE 7: Best-fit simulations of copper first coordination sphere EXAFS from the eight resting-state cytochrome c oxidase samples generated as in Figure 6c (- - -). (a) Simulations for data collected at 190 K (samples HB/Ua, HB/M, HB/P, vB/A). (b) Simulations for data collected at 4 K (samples HB/Ub, K/Bm, K/Bd, Y/E). For either temperature, the differences among simulations for different samples are about the same size or smaller than the noise in the raw EXAFS data (cf. Figure 4).

and fully reduced derivatives), allowing the assignment of most of the S-containing ligands to the Cu_A site (Scott, 1982).

Since it has been suggested that Cu_B is a "blue" copper (Powers et al., 1979), the possible existence of a short (2.11-2.18 Å) Cu-S interaction was investigated by including another Cu-S shell in the first-shell simulation for each of the eight resting-state samples. In the curve-fitting, the distance for this Cu-S shell was initially chosen as 2.15 Å and then

Table II: Curve-Fitting Results for the Outer Coordination Sphere of Resting-State Cytochrome c Oxidase Samples[a]

| sample | T (K) | Cu⋯C | | | Cu⋯Fe | | | f' |
		N_s	R_{as} (Å)	$\Delta\sigma_{as}^2$ (Å²)	N_s	R_{as} (Å)	$\Delta\sigma_{as}^2$ (Å²)	
HB/Ua	190	(4)[b]	2.96 ± 0.01	0.0017 + 0.0016 − 0.0010	(0.5)	3.03 ± 0.04	0.0079 + 0.0065 − 0.0033	0. 423
HB/M	195	(4)	2.95 ± 0.01	0.0019 + 0.0015 − 0.0010	(0.5)	3.02 ± 0.04	0.0105 + 0.0082 − 0.0041	0.0323
HB/P	190	(4)	2.94 ± 0.01	0.0007 + 0.0017 − 0.0010	(0.5)	2.99 ± 0.03	0.0049 + 0.0047 − 0.0028	0.0360
vB/A	190	(4)	2.93 ± 0.01	0.0023 + 0.0017 − 0.0012	(0.5)	2.99 ± 0.04	0.0026 + 0.0029 − 0.0018	0.0410
HB/Ub	4	(4)	2.94 ± 0.01	0.0011 + 0.0014 − 0.0010	(0.5)	3.04 ± 0.03	0.0056 + 0.0041 − 0.0025	0.0309
K/Bm	4	(4)	2.93 ± 0.01	0.0016 + 0.0018 − 0.0011	(0.5)	2.97 ± 0.03	0.0061 + 0.0053 − 0.0029	0.0354
K/Bd	4	(4)	2.91 ± 0.01	0.0024 + 0.0019 − 0.0013	(0.5)	2.97 ± 0.02	0.0016 + 0.0027 − 0.0017	0.0427

[a] N_s is the number of scatterers per copper; R_{as} is the copper-scatterer distance; $\Delta\sigma_{as}^2$ is defined as in Table I with references [Cu(mnt)₂]²⁻ at 4 K for Cu⋯C and [Fe(TPP)]₂[Cu(mnt)₂] at 4 K for Cu⋯Fe. [b] Numbers in parentheses were not varied during optimizations.

allowed to vary along with σ_{as}^2 during the optimization. The resulting optimized simulations in many cases assigned chemically unreasonable distances (1.8–2.0 Å) to this second Cu–S interaction and in all cases gave insignificant improvement in the fit (f' decreased by about 20%). Thus, inclusion of a short Cu–S interaction is unnecessary to adequately fit the first coordination sphere data.

A detailed analysis of the third peak (at $R' \simeq 2.7$ Å) in the Fourier transforms of the Cu EXAFS of these resting-state samples was performed by Fourier filtering this peak separately, as exemplified in Figure 6a,d,e. This FT peak falls at a distance expected for "second-shell" carbons (C₂,C₄) of imidazole ligands (from histidines) (Co et al., 1981), but it cannot be assigned solely to C scattering as we have previously demonstrated (Scott et al., 1986). This conclusion is based on observation of significant differences in the phases of the EXAFS oscillations giving rise to this peak in the cytochrome c oxidase samples compared to a peak at $R' \simeq 2.7$ Å in the FT of [Cu(imidazole)₄]²⁺. We assign a significant portion of this FT peak in the cytochrome c oxidase samples to Cu⋯Fe scattering (within the Cu$_B$–Fe$_{a_3}$ binuclear site), and the curve-fitting results described here corroborate that assignment. These fits are summarized in Table II for seven of the eight resting-state samples. Sample Y/E does not show a significant FT peak at this distance (cf., Figure 5h) and thus was not included in the analysis. Although this could be interpreted in terms of a difference in the structure of the binuclear site in the Yonetani preparation, it should also be noted that the data for sample Y/E exhibit considerably more noise than the other samples (as reflected in the artifactual peaks at high R' in Figure 5h), and this may result in obscuring the FT peak at $R' = 2.7$ Å.

The fits in Table II are two-shell fits using one shell of Cu⋯Fe and one shell of Cu⋯C interactions. Curve-fitting using only Cu⋯Fe or only Cu⋯C resulted in f' values that were worse (higher) than those reported in Table II by a factor of 2–4. The number of Cu⋯Fe interactions was fixed at 1 (per two coppers), and the number of Cu⋯C interactions was arbitrarily selected to be 8 (i.e., four imidazole ligands each with two carbons) distributed between two coppers, since the number of imidazoles within the 6 ± 1 Cu–(N,O) ligands is not known. (The fitting results are not sensitive to this number, since choosing a higher number is just compensated by a higher resulting $\Delta\sigma_{as}^2$ for the Cu⋯C shell.) As in the copper first-coordination sphere analysis, the results of these fits differ very little from sample to sample. The average Cu⋯C distance (2.94 ± 0.01 Å) is close to that expected for imidazole ligation

(3.0 Å) (McFadden et al., 1976). The average Cu⋯Fe distance is 3.00 ± 0.03 Å, which disagrees with the value for the Cu$_B$⋯Fe$_{a_3}$ distance of 3.8 Å reported by Powers et al. (1981). If such an interaction were present, it would give rise to an FT peak at $R' \simeq 3.5$ Å, yet we observe no reproducible feature in the Fourier transforms of these samples at that distance (especially in the 4 K data, for which one might expect an enhancement of such a long distance interaction).

CONCLUSIONS

Examination of the Cu K absorption edge and EXAFS of resting-state cytochrome c oxidase samples prepared by several different methods has allowed the following conclusions regarding the molecular and electronic structure of the copper sites in this enzyme:

(1) The unusual position and shape of the copper edge may adequately be explained by the presence of sulfur-containing ligands resulting in S → Cu(II) charge transfer, which has also been suggested to give rise to the unique EPR spectrum of Cu$_A$ (Blair et al., 1983; Hoffman et al., 1980).

(2) There is no convincing evidence from either copper edge or EXAFS data for the existence of a blue copper site in cytochrome c oxidase.

(3) Although the major Cu EXAFS Fourier transform peaks appear to vary from one resting-state sample to another, quantitative curve-fitting analysis indicates that there are no significant differences in the average copper first-coordination sphere structures among samples prepared by different methods.

(4) The major portion of the first coordination spheres of Cu$_A$ and Cu$_B$ consists of the following ligands (per two coppers): 6 ± 1 nitrogens (or oxygens) at an average copper-ligand distance of 1.99 ± 0.03 Å and 2 ∓ 1 sulfurs at an average copper–sulfur distance of 2.28 ± 0.02 Å.

(5) The Fourier transform peak at $R' \simeq 2.7$ Å is assigned partially to a Cu⋯Fe interaction, and curve-fitting results indicate that the Cu$_B$⋯Fe$_{a_3}$ distance is 3.00 ± 0.03 Å.

With this information and considering other spectroscopic evidence, Figure 8 has been constructed as our "best guess" for the structures of the copper active sites in resting-state cytochrome c oxidase. The hypothesized structures in Figure 8 incorporate evidence from ENDOR and EPR investigations of isotopically labeled yeast enzyme indicating the presence of at least one histidine and one cysteine in the Cu$_A$ coordination sphere (Blair et al., 1983). Our earlier XAS work (Scott, 1982) comparing fully reduced and mixed valence derivatives with the resting enzyme suggested the presence of
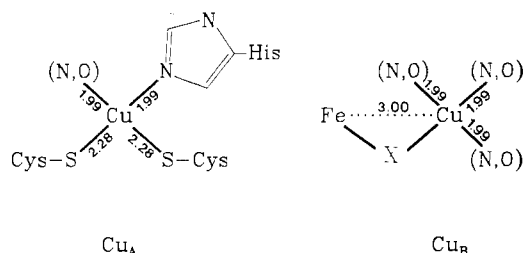
FIGURE 8: Hypothesized structures for the two copper sites in resting-state cytochrome *c* oxidase based on XAS data presented herein and on other spectroscopic data. (N,O) means that either N or O could be bound to Cu. The numbers given are average interatomic distances in Å. It is possible that one S-containing ligand is bound to Cu_B in place of an (N,O)-containing ligand.

two sulfur-containing ligands at the Cu_A site with approximately equivalent Cu–S distances. The resulting structure is expected to be covalent enough to yield the very small copper hyperfine splitting observed in the EPR spectrum. Assignment of two Cu–S interactions to the Cu_A site results in our suggestion of all (N,O)-containing ligands at the Cu_B site, as shown in Figure 8, although the possibility of one Cu–S interaction at Cu_B cannot be completely ruled out.

Our conclusions regarding the structures of the resting-state active sites disagree in some respects with those presented by Powers, Chance, and co-workers. The differences are most significant for the binuclear site, for which Powers et al., suggest a sulfur-containing bridge and a 3.8-Å $Cu_B \cdots Fe_{a_3}$ separation in work performed on enzyme prepared by the Yonetani method (Chance & Powers, 1985; Chance et al., 1981; Powers & Chance, 1984; Powers et al., 1981). Since we were unable to analyze the data on our sample of enzyme prepared by the Yonetani method for a Cu⋯Fe distance, the possibility still exists that the major resting-state enzyme form exhibits a different binuclear site structure when prepared by the Yonetani method as compared to the other preparation methods examined in this study. This difference may also be reflected in the differing cyanide-binding reactivity among the various preparations (Naqui et al., 1984). It should be emphasized that there is no disagreement that the sulfur-bridged binuclear site is a physiologically inactive form. Activated forms of cytochrome *c* oxidase evidently do not exhibit such a structure (Chance & Powers, 1985). It is our belief that the binuclear site structure reported in this study more closely resembles the physiologically relevant structure. We are currently involved in similar studies on activated enzyme forms to test this hypothesis.

REFERENCES

Addison, A. W., & Sinn, E. (1983) *Inorg. Chem. 22*, 1225–1228.

Blair, D. F., Martin, C. T., Gelles, J., Wang, H., Brudvig, G. W., Stevens, T. H., & Chan, S. I. (1983) *Chem. Scr. 21*, 43–53.

Brudvig, G. W., Stevens, T. H., Morse, R. H., & Chan, S. I. (1981) *Biochemistry 20*, 3912–3921.

Brunori, M., Colosimo, A., Rainoni, G., Wilson, M. T., & Antonini, E. (1979) *J. Biol. Chem. 254*, 10769–10775.

Chance, B., & Powers, L. (1985) *Curr. Top. Bioenerg. 14*, 1–19.

Chance, B., Powers, L., & Ching, Y. (1981) in *Mitochondria and Microsomes* (Lee, C. P., Schatz, G., & Dallner, G., Eds.) pp 271–292, Addison-Wesley, London.

Co, M. S., Scott, R. A., & Hodgson, K. O. (1981) *J. Am. Chem. Soc. 103*, 986–988.

Colosimo, A., Brunori, M., Sarti, P., Antonini, E., & Wilson, M. T. (1981) *Isr. J. Chem. 21*, 30–33.

Cramer, S. P., & Scott, R. A. (1981) *Rev. Sci. Instrum. 52*, 395–399.

Davison, A., & Holm, R. H. (1967) *Inorg. Synth. 10*, 8–26.

Elliott, C. M., & Akabori, K. (1982) *J. Am. Chem. Soc. 104*, 2671–2674.

Froncisz, W., Scholes, C. P., Hyde, J. S., Wei, Y.-H., King, T. E., Shaw, R. W., & Beinert, H. (1979) *J. Biol. Chem. 254*, 7482–7484.

Glick, M. D., Gavel, D. P., Diaddario, L. L., Rorabacher, D. B. (1976) *Inorg. Chem. 15*, 1190–1193.

Hartzell, C. R., Beinert, H., van Gelder, B. F., & King, T. E. (1978) *Methods Enzymol. 53*, 54–66.

Hoffman, B. M., Roberts, J. E., Swanson, M., Speck, S. H., & Margoliash, E. (1980) *Proc. Natl. Acad. Sci. U.S.A. 77*, 1452–1456.

Hu, V. W., Chan, S. I., & Brown, G. S. (1977a) *Proc. Natl. Acad. Sci. U.S.A. 74*, 3821–3825.

Hu, V. W., Chan, S. I., & Brown, G. S. (1977b) *FEBS Lett. 84*, 287–290.

Karlin, K. D., Dahlstrom, P. L., Hyde, J. R., & Zubieta, J. (1980) *J. Chem. Soc., Chem. Commun.*, 906–908.

Lee, P. A., Citrin, P. H., Eisenberger, P., & Kincaid, B. M. (1981) *Rev. Mod. Phys. 53*, 769–806.

MacGillavry, C. H., & Rieck, G. D. (1968) in *International Tables for X-Ray Crystallography*, Vol. 3, p 171, Kynoch, Birmingham.

McFadden, D. L., McPhail, A. T., Garner, C. D., & Mabbs, F. E. (1976) *J. Chem. Soc., Dalton Trans.*, 47–52.

Nalecz, K. A., Bolli, R., & Azzi, A. (1983) *Biochem. Biophys. Res. Commun. 114*, 822–828.

Naqui, A., Kumar, C., Ching, Y.-C., Powers, L., & Chance, B. (1984) *Biochemistry 23*, 6222–6227.

Orii, Y., & Okunuki, K. (1963) *J. Biochem. (Tokyo) 53*, 489–499.

Plumlee, K. W., Hoffman, B. M., Ibers, J. A., & Soos, Z. G. (1975) *J. Chem. Phys. 63*, 1926–1942.

Powers, L., & Chance, B. (1984) in *EXAFS and Near Edge Structure III* (Hodgson, K. O., Hedman, B., & Penner-Hahn, J. E., Eds.) pp 117–123, Springer-Verlag, Berlin.

Powers, L., Blumberg, W. E., Chance, B., Barlow, C. H., Leigh, J. S., Smith, J., Yonetani, T., Vik, S., & Peisach, J. (1979) *Biochim. Biophys. Acta 546*, 520–538.

Powers, L., Chance, B., Ching, Y., & Angiolillo, P. (1981) *Biophys. J. 34*, 465–498.

Schauer, C. K., Akabori, K., Elliott, C. M., & Anderson, O. P. (1984) *J. Am. Chem. Soc. 106*, 1127–1128.

Scott, R. A. (1982) in *The Biological Chemistry of Iron* (Dunford, H. B. Dolphin, D. H., Raymond, K. N., & Sieker, L. C., Eds.) pp 475–484, D. Reidel, Boston.

Scott, R. A. (1985) *Methods Enzymol. 117*, 414–459.

Scott, R. A., & Dooley, D. M. (1985) *J. Am. Chem. Soc. 107*, 4348–4350.

Scott, R. A., Cramer, S. P., Shaw, R. W., Beinert, H., & Gray, H. B. (1981) *Proc. Natl. Acad. Sci. U.S.A. 78*, 664–667.

Scott, R. A., Schwartz, J. R., & Cramer, S. P. (1984) in *EXAFS and Near Edge Structure III* (Hodgson, K. O., Hedman, B., & Penner-Hahn, J. E., Eds.) pp 111–116, Springer-Verlag, Berlin.

Scott, R. A., Schwartz, J. R., & Cramer, S. P. (1986) in *Biological and Inorganic Copper Chemistry* (Karlin, K. D., & Zubieta, J., Eds.) Vol. I, pp 41–52, Adenine Press, New York.

Sugiura, Y., Hirayama, Y., Tanaka, H., & Ishizo, K. (1975) *J. Am. Chem. Soc. 97*, 5577–5581.

Teo, B.-K., & Lee, P. A. (1979) *J. Am. Chem. Soc. 101*, 2815–2832.

Wikström, M., Krab, K., & Saraste, M. (1981) in *Cytochrome Oxidase. A Synthesis*, Academic Press, New York.

Yonetani, T. (1961) *J. Biol. Chem. 236*, 1680–1688.

Environmental Modulation of C-Terminus Dynamic Structure in Bacteriorhodopsin[†]

Jeffrey Marque,*,[‡] Kazuhiko Kinosita, Jr.,[‡] Rajni Govindjee,[§] Akira Ikegami,[‡] T. G. Ebrey,[§] and Jun Otomo[‡]

Institute of Physical and Chemical Research, Hirosawa, Wako-shi, Saitama 351-01, Japan, and Department of Physiology and Biophysics, University of Illinois at Urbana–Champaign, Urbana, Illinois 61801

ABSTRACT: We used steady-state and time-resolved (pulsed) fluorescence spectroscopies to study the dynamic structure of the COOH terminus in bacteriorhodopsin. The extrinsic fluorophore 8-aminonaphthalene-1,3,6-trisulfonic acid was attached to the protein, in purple membrane sheets, with a water-soluble carbodiimide; about 50% of the dye molecules were found to be attached to the COOH terminus. Signals from samples treated with papain were subtracted from non-papain-treated sample signals to give information about the COOH-terminus dynamics. Dye molecules on the COOH terminus fluoresce more strongly than dye molecules bound elsewhere on the membrane. This result, combined with our calculations showing that retinal is an energy acceptor in our system, suggests that the C-terminus spends most of its time away from the membrane surface. We systematically studied the effects of temperature, ionic strength, and pH, fitting the time-resolved anisotropy to $r(t) = r_\infty + (r_0 - r_\infty)e^{-t/\phi}$; the following picture emerged: In the pH range 5.6–10.9, raising the pH has the effect of increasing the fluorescence intensity and decreasing r_∞. We interpret this result to mean that the time-averaged position of the COOH terminus becomes farther from retinal as the pH is raised and that the range of Brownian motions of the C-terminus increases along with the pH. At pH 6.6, adding NaCl up to a concentration of 10 mM had qualitatively the same effects as raising the pH. Over the temperature range 10–50 °C, the time constant for anisotropy decay scales closely with the viscosity of water, a result consistent with Brownian motions of the COOH terminus in bulk water. We invariably found that $r_0 > 2r_\infty$. All of our results are consistent with the conclusion of Wallace and Henderson [Wallace, B. A., & Henderson, R. (1982) *Biophys. J. 39*, 233] that the COOH terminus of bacteriorhodopsin is free to assume many positions.

Bacteriorhodopsin (bR) is the sole protein constituent of purple membrane (PM), the light-driven proton pump that is part of the cell membrane in some strains of *Halobacterium halobium*. Bacteriorhodopsin is a single polypeptide containing seven α-helices that span the membrane; the final 20–25 amino acid residues at the carboxy terminus can be cleaved by papain digestion. These facts, plus further details on the structure and function of bR and PM, are covered in several review articles (Stoeckenius et al., 1979; Stoeckenius & Bogomolni, 1982; Dencher, 1983).

We have studied the dynamic structure of the carboxy terminus via steady-state and time-resolved fluorescence depolarization spectroscopy techniques. We are particularly interested in the pH and ionic strength dependence of the dynamic structure because pH and salt concentration are known to affect the kinetics of the proton pump and photocycle (Ort & Parson, 1978; Li et al., 1984; Govindjee et al., 1980). Although this is hardly surprising behavior in a proton pump, the mechanism of the effect is not yet established. A priori, the pH effect could simply be a concentration (of protons) effect, but we shall show in this paper that both the freedom of motion of the C-terminus and its distance from the membrane surface are, under some conditions, affected by the pH and ionic strength of the suspending medium.

Renthal et al. (1983) published the first fluorescence study of the bR C-terminus mobility. They attached the fluorophore danzylhydrazine to PM with a water-soluble carbodiimide, and they found that most of the probe was attached to the C-terminus. At a pH of 8.0 [0.05 M tris(hydroxymethyl)-aminomethane (Tris)], they found that the steady-state po-

* Address correspondence to this author at the School of Applied and Engineering Physics, Cornell University, Ithaca, NY 14853.

[‡] Institute of Physical and Chemical Research.

[§] University of Illinois at Urbana–Champaign.